

A POSSIBLE CORRELATION BETWEEN SUPPRESSION OF SUPERCONDUCTIVITY, MAGNETIC ORDERING AND NORMAL STATE RESISTIVITY PARAMETERS IN THE $\text{Yb}_{1-x}\text{Pr}_x\text{Ba}_2\text{Cu}_3\text{O}_{7-\delta}$ SYSTEM

ANURAG GUPTA*, H. NARAYAN*, P. N. LISBOA-FILHO[†], C. A. CARDOSO[‡],
FERNANDO M. ARAUJO MOREIRA[†], O. F. DE LIMA[‡] and A. V. NARLIKAR^{*,†}

* National Physical Laboratory, K.S. Krishnan Road, New Delhi 110012, India

[†] Universidade Federal de Sao Carlos, 13565-905 Sao Carlos, Brazil

[‡] Instituto de Fisica “Gleb Wataghin”, Universidade Estadual de Campinas-Unicamp,
13083-970 Campinas, SP, Brazil

Received 13 November 2001

Revised 5 April 2002

Polycrystalline samples of the Pr doped $\text{Yb}_{1-x}\text{Pr}_x\text{Ba}_2\text{Cu}_3\text{O}_{7-\delta}$ (i.e. Yb(Pr)-123) system for $0 \leq x \leq 1$ have been investigated for resistivity ρ and magnetization M as a function of temperature in normal and superconducting states. The gradual decrease in superconducting critical temperature $T_c(x)$ is found to be correlated with the x -dependent ratio of resistivity slope $(d\rho/dT)_{cc}$ (corresponding to the linear $\rho(T)$ region) and residual resistivity ρ_0 . In particular, the observed difference of critical Pr concentration where superconductivity is destroyed (x_c) in Yb(Pr)-123 ($x_c \approx 0.65$) and Y(Pr)-123 ($x_c \approx 0.55$) matches with the difference in the value of Pr concentration where the ratio $(d\rho/dT)_{cc}/\rho_0$ tends to go to zero in them. The $M(T)$ data of the Yb(Pr)-123 samples show magnetic ordering for $x > x_c$ at characteristic temperatures, T_n , that increase with x . Interestingly, the Yb(Pr)-123 sample with Pr content ($x = 0.6$) near x_c reveals several anomalous features like transition from metallic to semiconducting-like $\rho(T)$, an excessive broadening of the diamagnetic transition and weakening of the $M(T)$ signal related to antiferromagnetic ordering of Pr ions. These observations can be consistently interpreted by assuming the presence of dynamically fluctuating striped phase in these systems.

PACS Number(s): 74.62.Dh, 74.72.Bk

1. Introduction

The evolution of superconductivity and magnetism in $R_{1-x}\text{Pr}_x\text{Ba}_2\text{Cu}_3\text{O}_{7-\delta}$ (i.e. $R(\text{Pr})$ -123, where $R = Y/\text{Rare Earth}$), and its dependence on R 's ionic radii, has been one of the most challenging and interesting issues of high temperature superconducting cuprates (HTSC).^{1–8} Both superconducting critical temperature (T_c) and Neel temperature (T_n , antiferromagnetic ordering of Pr ions) tend to go to zero at a critical Pr concentration (x_c), and take their maximum values $x = 0$ and 1, respectively. A decrease in R 's ionic radii (as one moves right in the Lanthanide series) leads to an increase in x_c . Hybridization of Pr-4f with O-2p⁹ of

CuO₂ planes has been one of the most sought after explanations for simultaneous destruction of superconductivity and a high T_n (~ 17 K for $x = 1$). However, the observed R 's ionic size dependence of x_c is counter-intuitive to a pure hybridization-based scenario. One attempt to understand this came from the theoretical model of Liechtenstein and Mazin.¹⁰ They suggested that with Pr substitution an additional band crossing the Fermi energy (E_F) grabs holes from the CuO₂ planes and its position depends on R 's ionic size. However, later, Mazin¹¹ attributed the observation of superconductivity in single crystals of pure Pr-123¹² to the same band, which does not include the Cu-3d of the CuO₂ planes and still awaits an experimental confirmation.

It may well be possible that the Pr-4f and O-2p hybridization might complement rather than decide the simultaneous destruction of superconductivity and appearance of magnetic order in the $R(\text{Pr})$ -123 system. An alternative understanding, assuming that superconductivity originates in CuO₂ planes even in pure Pr-123 like other HTSC, may come from the proposed model of suppression of superconductivity by pinning of the dynamically fluctuating striped phase.^{13–17} There has been experimental evidence (see Ref. 17 and references therein) of the striped phase in general in HTSC including the R -123 system. In substituted R -123 systems, we recently¹⁸ observed a correlation between T_c and various normal state transport parameters, like residual resistivity (ρ_0) and temperature derivative of resistivity $(d\rho/dT)_{cc}$ in the high temperature linear region, that also supported the presence of the dynamic striped phase in R -123. In the present work, we look for a similar correlation in Yb(Pr)-123 and try to understand the possible source of simultaneous destruction of superconductivity and origin of magnetic ordering at x_c in it.

2. Experimental Details

Polycrystalline samples of the series Yb_{1-x}Pr_xBa₂Cu₃O_{7- δ} , with x ranging from 0 to 1, were synthesized through a solid state reaction method. The ingredients Yb₂O₃, Pr₆O₁₁, BaCO₃ and CuO of 4 N purity were thoroughly mixed in required proportions and calcined at 860°–910°C in air for a period of 24 hours. This exercise was repeated three times with intermediate grinding at each stage. The resulting powders were ground, mixed and pelletized. The pellets were annealed in flowing oxygen at 950°C for a period of 24 hours, followed by furnace cooling to room temperature with an intervening annealing for 48 hours at 600°C. The latter step ensures the total oxygen content $7 - \delta \approx 7$ in all the samples.¹⁹ The samples were then characterized for their phase purity and lattice parameters by X-ray diffraction. The resistance measurements were obtained using the standard four-probe technique. The DC magnetization as a function of temperature (1.5 to 100 K) was measured using a commercial squid-magnetometer in the field range of 0–50 kOe. Special care was taken to avoid residual fields while taking squid measurements. A flux gate was always used before a set of measurements, and between consecutive runs the sample was always heated up to 150 K to erase its previous magnetic

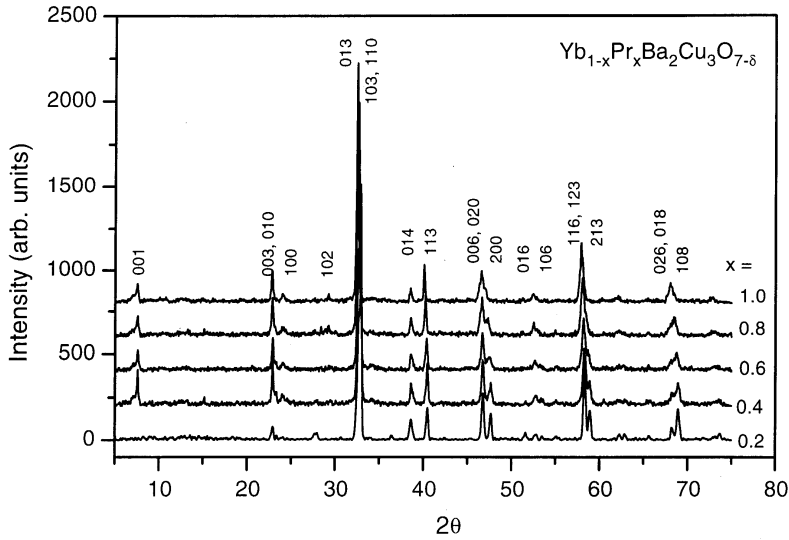


Fig. 1. X-ray diffraction patterns for various x values in $\text{Yb}_{1-x}\text{Pr}_x\text{Ba}_2\text{Cu}_3\text{O}_{7-\delta}$.

history, and then cooled down to the starting temperature in the absence of magnetic fields.

3. Experimental Results

Owing to the small ionic size of Yb as compared to most other rare-earths, the X-ray pattern of pure Yb-123 generally shows a few low intensity impurity peaks. Interestingly however, our present studies revealed that substitution of Yb by the larger Pr ion resulted in a phase pure material. As depicted in Fig. 1, the X-ray patterns of Yb(Pr)-123 with varying x show the single phase nature of the samples. Table 1 shows the variation of lattice parameters a , b and c , and orthorhombic distortion for all values of x . The increase of c -axis parameter with Pr indicates the substitution of larger Pr^{3+} ions (1.14 \AA) in the place of smaller Yb^{3+} ions (0.98 \AA). For all values of x the samples show an orthorhombic structure. However, with an increase in x (see Table 1) the orthorhombic distortion decreases monotonically. The evolution of the crystallographic splittings (see Fig. 1), for instance $[020]$, $[200]$ and $[123]$, $[213]$ supports the change in the orthorhombic distortion. It is also worth pointing out that, for a change in x from 0 to 1, the c -axis increases by 0.08 \AA in the case of Yb(Pr)-123 as compared to 0.04 \AA for Y(Pr)-123.¹⁹ This may indicate that, due to a smaller size of the Yb^{3+} ion (0.98 \AA) in comparison to the Y^{3+} ion (1.02 \AA), the enveloping CuO_2 planes in the former case are relatively compressed for $x < 1$.

Figure 2 shows the normalized resistivity (ρ/ρ_{300}) as a function of temperature for all the samples of Yb(Pr)-123. As is evident from the figure, the $\rho(T)$ behavior

Table 1. Lattice parameters (in Å) a , b and c , and orthorhombic distortion ($OD = [(b - a)/b] \times 100$) for the $\text{Yb}_{1-x}\text{Pr}_x\text{Ba}_2\text{Cu}_3\text{O}_{7-\delta}$ system.

x	a	b	c	OD
0	3.80326	3.87311	11.6433	1.8035
0.1	3.80472	3.87534	11.6425	1.8223
0.2	3.80950	3.87649	11.6477	1.7281
0.3	3.81653	3.88025	11.6578	1.6422
0.4	3.82074	3.88449	11.6677	1.6411
0.5	3.83080	3.88215	11.6797	1.3227
0.6	3.83464	3.88714	11.6824	1.3506
0.7	3.84709	3.89292	11.6994	1.1773
0.8	3.85670	3.89522	11.7028	0.9889
0.9	3.86585	3.89501	11.7312	0.7487
1.0	3.87991	3.90213	11.7279	0.5694

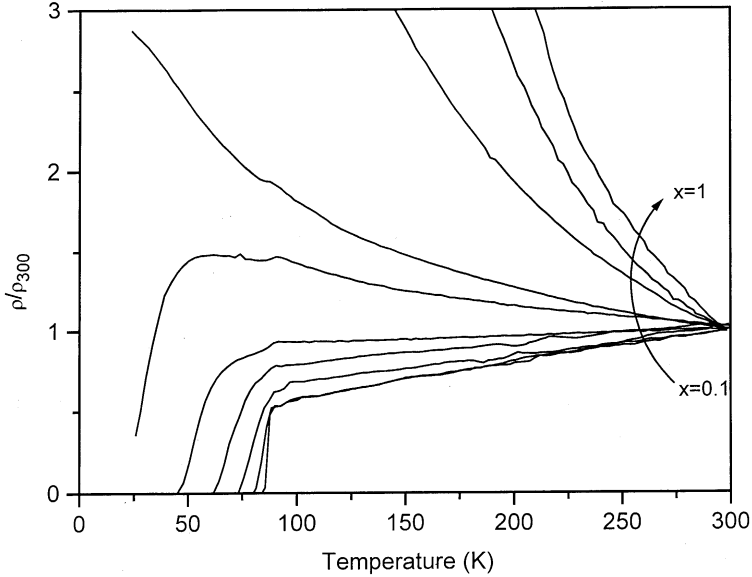


Fig. 2. Reduced resistivity (ρ/ρ_{300}) as a function of temperature for various x values (from 0.1 to 1 in steps of 0.1) in $\text{Yb}_{1-x}\text{Pr}_x\text{Ba}_2\text{Cu}_3\text{O}_{7-\delta}$.

anomalously changes from metallic to semiconductor-like for values of $x \geq 0.6$. All samples with $x \leq 0.6$ show a transition to superconducting state. Figure 3 shows the variation of reduced critical temperature $T_c(x)/T_c(0)$ with Pr concentration. Similar data, taken from the literature, for the $\text{Y}(\text{Pr})$ -123 system of both polycrystalline material^{5,19} and single crystals²⁰ are also plotted in the same figure. Slightly lower values of $T_c(\rho = 0)$ for single crystals reported in Ref. 20 are mainly due to tail-like broadening of $\rho(T)$ when ρ goes to zero. It is clear from the Fig. 3 that suppression of $T_c(x)$ for $\text{Yb}(\text{Pr})$ -123 is slower compared to $\text{Y}(\text{Pr})$ -123. The extrapolated value of

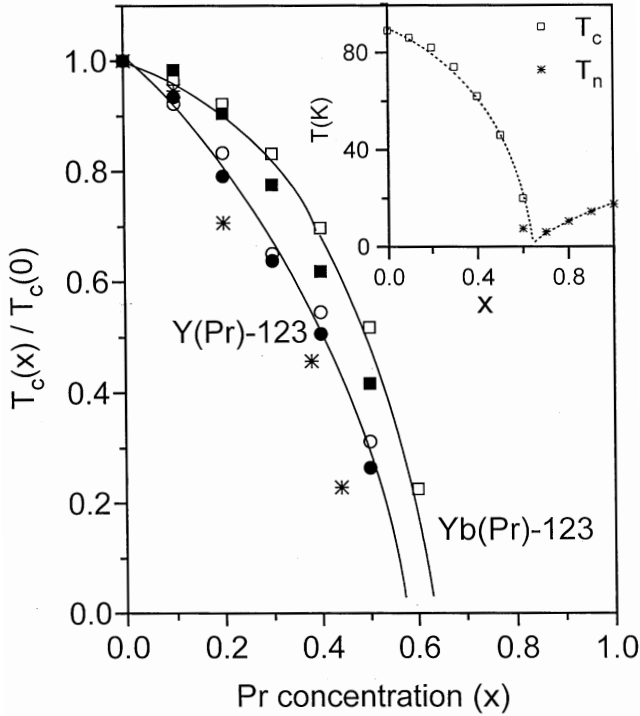


Fig. 3. Reduced critical temperature $T_c(x)/T_c(0)$ as a function of Pr concentration x in $\text{Yb}_{1-x}\text{Pr}_x\text{Ba}_2\text{Cu}_3\text{O}_{7-\delta}$ (present work), $\text{Y}_{1-x}\text{Pr}_x\text{Ba}_2\text{Cu}_3\text{O}_{7-\delta}$ (filled circles¹⁹ and open circles⁵) and single crystal $\text{Y}_{1-x}\text{Pr}_x\text{Ba}_2\text{Cu}_3\text{O}_{7-\delta}$ (stars²⁰). In the former, the T_c determination by both $\rho = 0$ (hollow squares) and diamagnetic onset (filled squares) are shown. Inset: $T_c(\rho = 0)$ and T_n as a function of x in $\text{Yb}_{1-x}\text{Pr}_x\text{Ba}_2\text{Cu}_3\text{O}_{7-\delta}$.

critical concentration of Pr to quench superconductivity x_c is ~ 0.65 for Yb(Pr)-123 and ~ 0.55 for the Y(Pr)-123 system. The observed increase of x_c with a decrease in R 's ionic size is in line with previous reports.¹⁻⁸

Figure 4 shows DC magnetization as a function of temperature, under an applied field $H = 10$ Oe, for Yb(Pr)-123 samples with $x = 0$ to 0.6. The magnetization data shown in Fig. 4 is normalized by M_{\min} (the minimum value of M observed at the low temperature side of the transition) to magnify the transitions for higher values of x . Values of M_{\min} , related with shielding fraction, decrease drastically with the increase in x (results not shown). It decreases by over 25 times for samples with $x = 0.6$ when compared to samples with $x = 0.1$. The incomplete Meissner effect and similar dependence of shielding fraction on doping in HTSC has been always observed (e.g. see Refs. 21 and 22) and are not yet completely understood. However, all the samples show a clear diamagnetic onset in $M(T)$, marking the superconducting transition. The $T_c(x)$ defined by the diamagnetic onset, also plotted in Fig. 3, shows a decrease with an increase in x similar to that measured resis-

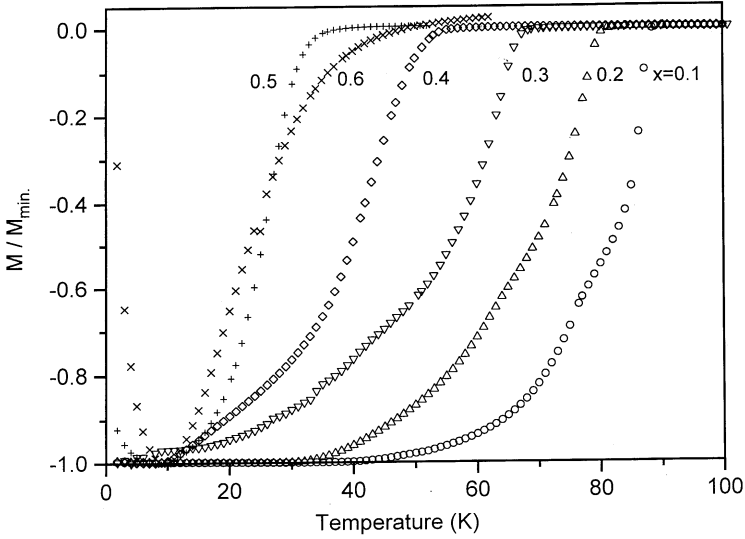


Fig. 4. Reduced magnetization (M/M_{\min}) in an applied field $H = 10$ Oe as a function of temperature for $x = 0$ to 0.6 in $\text{Yb}_{1-x}\text{Pr}_x\text{Ba}_2\text{Cu}_3\text{O}_{7-\delta}$.

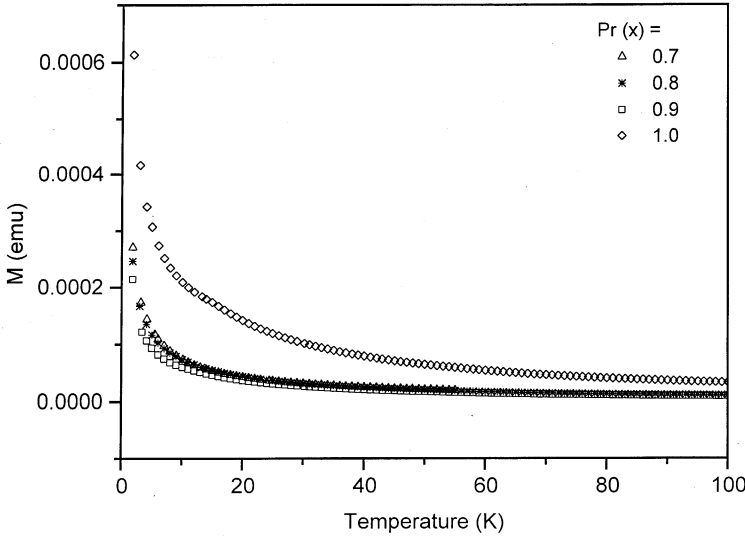


Fig. 5. Magnetization in an applied field $H = 10$ Oe as a function of temperature for $x = 0.7$ to 1.0 in $\text{Yb}_{1-x}\text{Pr}_x\text{Ba}_2\text{Cu}_3\text{O}_{7-\delta}$.

tively. However, the diamagnetic onset for the $x = 0.6$ sample was expected at a temperature lower than that for the $x = 0.5$ sample, whereas the observed behavior is found contrary to that (see Fig. 4). This shows that for the $x = 0.6$ sample the diamagnetic onset has become anomalously broad. For samples with $x = 0.7$ to 1.0

the $M(T)$ plots (see Fig. 5), under an applied field $H = 10$ Oe, follow a Curie-Weiss-like behavior and show no trace of superconductivity down to under 1.5 K. It is already known¹⁻⁸ that the non-superconducting $R(\text{Pr})$ -123 system shows an antiferromagnetic ordering of Pr ions at a characteristic temperature $T_n(x)$. For our $x = 1$ sample one could easily notice an anomaly corresponding to T_n at 17 K which became clear by plotting dM/dT versus T . But for the other three samples of Fig. 5 the same was not so apparent. Following the work of Ref. 8, besides plotting dM/dT we tried also, by plotting M^{-1} versus T and $\log(M)$ versus $\log(T)$, to extract the $T_n(x)$ values from the $M(T)$ data. $T_n(x)$ values were most conspicuous only in the $\log(M)$ versus $\log(T)$ plot, where a change in the slope for all the samples with $x \geq 0.7$ was observed (see Fig. 6(a)). The change in the slopes are also visible as peaks, typically observed at slightly lower (by ~ 3 K) temperatures, in the plots of

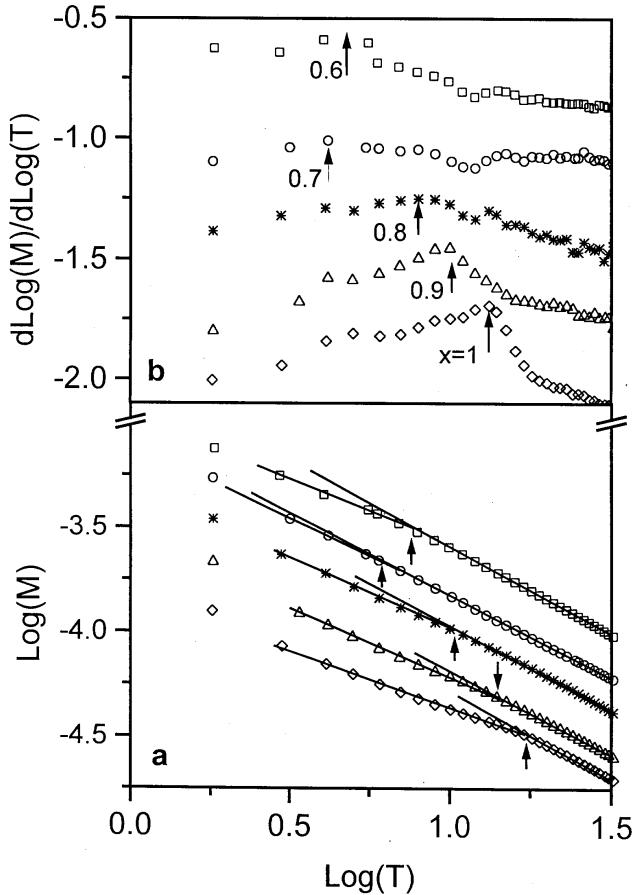


Fig. 6. (a) $\log(M)$ versus $\log(T)$ and (b) $d\log(M)/d\log(T)$ versus $\log(T)$ for various x values in $\text{Yb}_{1-x}\text{Pr}_x\text{Ba}_2\text{Cu}_3\text{O}_{7-\delta}$. M for $x = 0.6$ is measured in an applied field $H = 10$ kOe (see text also), whereas for all other samples $H = 10$ Oe.

$d\log(M)/d\log(T)$ versus $\log(T)$ (see Fig. 6(b)). The values of $T_n(x)$ (see inset of Fig. 3) corresponding to the change in slope, and their increase is in accord with the general trend reported for the $R(\text{Pr})$ -123 system.¹⁻⁸

The superconducting samples of $\text{Yb}(\text{Pr})$ -123 with $x = 0.5$ and 0.6 also showed upturns in $M(T)$ at low temperatures (see Fig. 4). These upturns presumably indicate the paramagnetic effect due to Pr ions competing with diamagnetism due to superconductivity. To check that the upturns are not due to magnetic ordering in these samples, the $M(T)$ measurements were carried out under high-applied fields up to 50 KOe. For instance, for the $x = 0.6$ sample, the $M(T)$ data under $H = 10$ kOe is also included in Fig. 6. Interestingly, we observe a break in the slope at a characteristic temperature that may apparently indicate a T_n . However, firstly, as seen from the inset of Fig. 3, this value of $T_n(x = 0.6)$ does not follow the same curve as that for non-superconducting samples with $x \geq 0.7$. Secondly, on closer inspection of the data in Fig. 6, we see that the change in slope of $\log(M)$ versus $\log(T)$ and the peak in $d\log(M)/d\log(T)$ plots at T_n gets weaker with the decrease in x until $x = 0.7$. However, for $x = 0.6$, there is a fresh enhancement in the break of the slope and the peak (see Fig. 6). Considering that the $x = 0.6$ sample is superconducting, this may actually indicate a diamagnetic decrease occurring at a lower temperature when $H = 10$ kOe as compared to that observed with smaller $H = 10$ Oe (see Fig. 4). Thirdly, the detailed heat capacity studies carried out in the temperature range of 2–15 K for this sample failed to show even a broad hump that could be related to T_n as coexisting with T_c . Thus, the break in $M(T)$ observed for superconducting samples needs to be considered only cautiously as far as magnetic ordering is concerned.

4. Discussion

We are looking for a possible correlation of T_c with residual resistivity (ρ_0) as extracted from the extrapolation of linear $\rho(T)$ region to $T = 0$ K and resistivity slope $(d\rho/dT)_{cc}$ corresponding to the linear $\rho(T)$ region in our $\text{Yb}(\text{Pr})$ -123 samples. However, considering the use of substituted polycrystalline samples in the present work, it is important to consider the possible extrinsic contributions that may interfere with the intrinsic values of these parameters in the material. We first discuss three such sources of error that may arise due to inhomogeneous substitution, the anisotropic nature of R -123 system and defects in the grain boundaries. Next, we delineate the intrinsic nature of ρ_0 and $(d\rho/dT)_{cc}$ in the $\text{Yb}(\text{Pr})$ -123 samples by a comparison with both polycrystalline and single crystalline $\text{Y}(\text{Pr})$ -123 samples, and discuss that how their correlation with T_c may indicate the presence of dynamically fluctuating striped phase as a common source of superconductivity and antiferromagnetism in these systems.

For a few results obtained in the present work, e.g. at higher values of x (> 0.2) the $T_c(x)$ determined by $\rho = 0$ is higher in comparison to that estimated by diamagnetic onset (see Fig. 3); the shielding fraction decreases with an increase in

Pr doping as mentioned in the experimental results; broad diamagnetic response below the onsets in $M(T)$ (see Fig. 4) seem to reveal something about the nature of superconductivity in our Yb(Pr)-123 samples. They probably indicate that, with increased Pr doping, higher T_c filamentary-superconducting paths start to evolve in the samples before a weak bulk superconductivity emerges at lower temperatures. This raises an important question — what is the origin of such superconductivity observed in our samples? Is it due to some macroscopic inhomogeneity, for instance, inhomogeneous cation (Pr, Yb) distribution along the Josephson-coupled grain boundaries? Or can it have some intrinsic origin? The former line of reasoning is apparently not supported by our XRD results, and the observed $T_c(x)$ and $T_n(x)$ behavior. The presence of inhomogeneous cation (Pr, Yb) distribution should lead to broadening of the XRD peaks that should enhance further with an increase in Pr, and no systematic change in lattice parameters should occur, which is not observed (see Fig. 1 and Table 1). Second, the systematic and expected^{1–8} decrease observed in $T_c(x)$ measured both by $M(T)$ and $\rho(T)$, and the emergence of $T_n(x)$, (see Fig. 3) is not accidental and is definitely connected with the intrinsic substitutional effects in the Yb(Pr)-123 system. Thus, we propose looking for answers that may be generic to highly doped HTSC and where microstructural details of the sample are irrelevant as far as the origin of superconductivity is concerned. Good starting points in this direction are offered by various models, for instance, of quantum percolation in the presence of nanolevel inhomogeneities²³ and tunneling of cooper pairs across the static striped phases¹⁷ (see below also).

Due to the anisotropic nature of HTSC, the measured resistivity in the polycrystalline sample seems to represent the sum of the contribution along and across the CuO_2 planes. However, we believe that the resistivity of the R -123 samples will be mainly determined by the transport along well-connected CuO_2 planes across the grain boundaries. This assumption follows from the fact that the resistivity of the R -123 system, due to anisotropy, is roughly 20 times smaller along the CuO_2 planes than along the c -axis (i.e. across the CuO_2 planes).²⁴ Moreover, as reported,²⁵ in the $R(\text{Pr})$ -123 system the anisotropy increases further with Pr doping. Thus, the main error may arise only from the microstructure dependent effective cross-sectional area and length for electrical transport in different samples. Considering the ratio of $(d\rho/dT)_{cc}/\rho_0$ should cancel out these geometrical factors. The third source of error, i.e. defects in the grain boundaries, may contribute to the temperature independent part of the resistivity, namely ρ_0 . This aspect can be cross-checked by a comparison with single crystal data, that we could find only for the Y(Pr)-123 system.²⁰ The ratio of $(d\rho/dT)_{cc}/\rho_0$ as a function of x is shown in Fig. 7 for polycrystalline Yb(Pr)-123 (present work) and Y(Pr)-123 (taken from Ref. 19), and single crystals of Y(Pr)-123 (taken from Ref. 20). Values of ρ_0 are extracted from the extrapolation of linear $\rho(T)$ region to $T = 0$ K, and thus represent only a lower limit to the true value. Due to an increasing curvature of $\rho(T)$ for single crystals with $x \geq 0.4$ in Ref. 20, the ratio could not be determined reliably for higher values of x . The data on Y(Pr)-123 single crystal samples had to be normalized

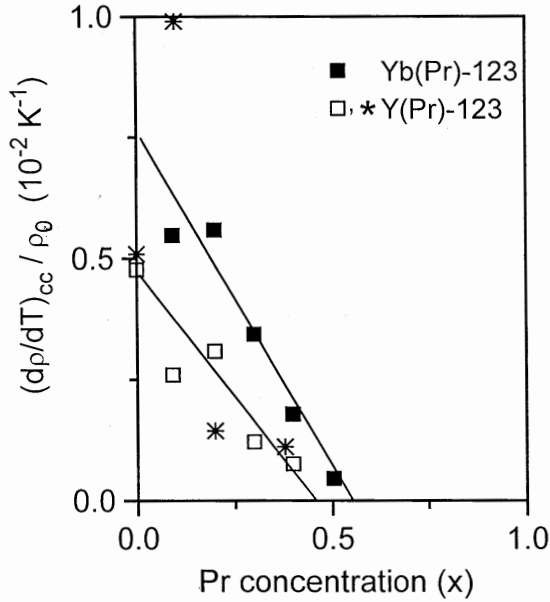


Fig. 7. Ratio of resistivity slope $(d\rho/dT)_{cc}$ and residual resistivity ρ_0 as a function of Pr concentration x in $\text{Yb}_{1-x}\text{Pr}_x\text{Ba}_2\text{Cu}_3\text{O}_{7-\delta}$ (filled squares represent present work), $\text{Y}_{1-x}\text{Pr}_x\text{Ba}_2\text{Cu}_3\text{O}_{7-\delta}$ (open squares¹⁹) and single crystals $\text{Y}_{1-x}\text{Pr}_x\text{Ba}_2\text{Cu}_3\text{O}_{7-\delta}$ (stars²⁰). The solid lines represent a linear fit of the data.

by a constant factor of four to match it with that of the polycrystalline samples in Fig. 7. This factor reveals a definite contribution of grain boundaries to ρ_0 , as mentioned above, in case of the latter samples. However, as seen in Fig. 7, the behavior of the polycrystalline samples does qualitatively resemble that of the single crystals, giving credence to the fact that the ratio of $(d\rho/dT)_{cc}/\rho_0$ in the former is indeed related to the intrinsic property of the material. From Figs. 7 and 3, we may thus infer two interesting observations: (a) the ratio $(d\rho/dT)_{cc}/\rho_0$ decreases with increasing x , in both $\text{Y}(\text{Pr})$ -123 and $\text{Yb}(\text{Pr})$ -123, as does the $T_c(x)$ in them; and (b) the ratio tends to go to zero at Pr concentration that is roughly 0.1 smaller for $\text{Y}(\text{Pr})$ -123 than $\text{Yb}(\text{Pr})$ -123, that also matches with the observed difference of x_c in them. These observations reveal a definite correlation of T_c with ρ_0 and $(d\rho/dT)_{cc}$ in these systems.

Now, we show that superconductivity due to dynamically fluctuating striped phase in CuO_2 planes can consistently explain the observed correlation of T_c with $(d\rho/dT)_{cc}/\rho_0$. The increase of residual resistivity ρ_0 reflects an increase of impurities/defects, which can suppress the superconductivity by pinning the fluctuating stripes. T_c should, as observed, correlate as inversely proportional to ρ_0 . On the other hand, the increase of resistivity slope $(d\rho/dT)_{cc}$ reflects either an increase in carrier concentration or an increase in carrier-carrier scattering. The increase of carrier density should amount to an increase in the density of charged stripes,

which we expect would then require larger disorder to get pinned. For the latter case, because now the source of scattering is a carrier itself that is mobile, we expect that it (the carrier) will tend to depin the striped phase. In both cases the increase of $(d\rho/dT)_{cc}$ will thus tend to relatively enhance T_c . The T_c should, as observed, correlate as directly proportional to $(d\rho/dT)_{cc}$. One may also say that, based on the decreasing ratio of $(d\rho/dT)_{cc}/\rho_0$ with x in Fig. 7, with an increase in Pr substitution, the dynamically fluctuating striped phase in CuO_2 planes slows down more and more. Above x_c the fluctuating striped phase may become static, which then leads to the ordering of the Pr ions by a mechanism involving hybridization of Pr-4f with O-2p of CuO_2 planes. And with increasing x (above x_c), a larger number of Pr ions participate in magnetic ordering to give an increasing $T_n(x)$, as seen in the inset of Fig. 3. It is tempting to conclude that x_c in the phase-diagram for $R(\text{Pr})$ -123 marks the transition from static to fluctuating charge dynamics in CuO_2 planes. As also seen in Fig. 2, the non-superconducting $\text{Yb}(\text{Pr})$ -123 samples with $x \geq 0.7$, i.e. just above and greater than $x_c \sim 0.65$, show an increasing tendency of exponentially dependent $\rho(T)$ at low temperatures. This may be an indication of inter/intra-charge hopping in a static striped phase.¹⁷ The superconducting sample with $x = 0.6$, i.e. just below $x_c \sim 0.65$, shows a negative $d\rho/dT$ along with a very broad diamagnetic onset extending much above its $T_c(\rho = 0) \sim 20$ K (see Figs. 2 and 4). This may reflect the precursor of a “spin-gap” at $T > T_c$ due to critical slowing down of fluctuating stripe dynamics in samples with x near and below x_c . This is corroborated by the fact that the diamagnetic onset becomes relatively sharp as one moves away and to smaller values of x (see Fig. 4). It may be interesting in future to study more samples with Pr concentration around and near to x_c . We would like to mention here that the observed unusual broadening of $M(T)$ for the $x = 0.6$ sample cannot be related with inhomogeneity in a straight forward way, as then it should have been present in all the superconducting samples, prepared in identical conditions, for values of $x \leq 0.6$, which is not the case.

Finally, we discuss a possible physical origin for the ionic-size dependence of x_c in $R(\text{Pr})$ -123. It may come from the dependence of anti-site substitution of Pr^{3+} at the Ba^{2+} site²⁶ and/or Pr^{4+} at R^{3+} site²⁷ on the ionic size of R . It was shown in $\text{Y}(\text{Pr})$ -123 single crystals that these aliovalent substitutions directly lead to the creation of oxygen vacancies in CuO_2 planes.²⁷ Such vacancies can be an important source of impurities in CuO_2 planes that can pin the fluctuating stripes. However, the impact of such anti-site substitution on $(d\rho/dT)_{cc}$ is not *a priori* clear, which needs to be studied in more detail for various $R(\text{Pr})$ -123 systems. In the present case, however, because of smaller ionic size of Yb the possibility of anti-site defect formation should be less in comparison to Pr substitution in Y -123.²⁷ Thus, comparatively the oxygen disorder is expected to be less as corroborated by the lattice parameter data, showing fewer O(5) sites getting filled-up. As a result the pinning of fluctuating stripes is less in $\text{Yb}(\text{Pr})$ -123 and the value of x_c is higher.

5. Conclusion

In summary, the gradual destruction of superconductivity with increasing Pr, in both Yb(Pr)-123 and Y(Pr)-123 systems, seems to show up in the change of normal state parameters ρ_0 and $(d\rho/dT)_{cc}$, which can be extracted from the $\rho(T)$ curves. In both cases, it is found that the ratio of $(d\rho/dT)_{cc}/\rho_0$ tends to decrease with increasing x as does the $T_c(x)$. The difference in the values of Pr concentration where this ratio tends to go to zero matches with the observed difference of x_c in them. Moreover, for the Pr content near x_c , several properties like $\rho(T)$, the diamagnetic onset in $M(T)$ and the antiferromagnetic ordering of Pr ions show anomalous behavior. These results can be consistently explained by the presence of dynamically fluctuating striped phase in them. The critical Pr concentration x_c in R(Pr)-123 probably marks a transition from dynamic to static striped phase, where simultaneously superconductivity gets destroyed and magnetic ordering of Pr ions originates.

Acknowledgments

The authors from UFSCar, Sao Carlos and UNICAMP, Campinas, Brazil, would like to thank the Brazilian funding agency FAPESP for providing partial financial support (including the maintenance of AVN) to carry out the present work. H. Narayan and A. V. Narlikar from NPL acknowledge Grant Nos. 31/1/(179)/2000-EMR-I and 21(0463)/99-EMR-II from CSIR.

References

1. L. Soderholm, K. Zhang, D. G. Hinks, M. A. Beno, J. D. Jorgensen, C. V. Segree and I. K. Schuller, *Nature* **328**, 604 (1987).
2. I. Felner, U. Yaron, I. Nowik, E. R. Bauminger, Y. Wolfus, E. R. Yacoby, G. Hilscher and N. Pillmayer, *Phys. Rev.* **B40**, 6739 (1989).
3. D. W. Cooke, R. S. Kwok, R. L. Lichti, T. R. Adams, C. Boekema, W. K. Dawson, A. Kebede, J. Schwegler, J. E. Crow and T. Mihalisin, *Phys. Rev.* **B41**, 4801 (1990).
4. Y. Xu and W. Guan, *Solid State Commun.* **80**, 105 (1991).
5. S. K. Malik, C. V. Tomy and P. Bhargava, *Phys. Rev.* **B44**, 7042 (1991).
6. H. B. Radousky, *J. Mat. Res.* **7**, 1917 (1992).
7. H. Jhans, S. K. Malik, S. K. Dhar and R. Vijayaraghavan, *Physica* **C207**, 247 (1993).
8. W. Guan, Y. Xu, S. R. Sheen, Y. C. Chen, J. Y. T. Wei, H. F. Lai, M. K. Wu and J. C. Ho, *Phys. Rev.* **B49**, 15993 (1993).
9. Fehrenbacher and T. M. Rice, *Phys. Rev. Lett.* **70**, 3471 (1993).
10. A. I. Liechtenstein and I. I. Mazin, *Phys. Rev. Lett.* **74**, 1000 (1995).
11. I. I. Mazin, *Phys. Rev.* **B60**, 92 (1999).
12. Z. Zou, J. Ye, K. Oka and Y. Nishihara, *Phys. Rev. Lett.* **80**, 1074 (1998).
13. G. D. Liu, Z. X. Zhao and G. C. Che, *Solid State Commun.* **109**, 495 (1999).
14. J. S. Zhou, J. B. Goodenough, H. Sato and M. Naito, *Phys. Rev.* **B59**, 3827 (1999).
15. R. F. Service, *Science* **283**, 1106 (1999).
16. N. Hasselmann, A. H. Castro Neto, C. Morair Smith and Y. Dimashko, *Phys. Rev. Lett.* **82**, 2135 (1999).
17. V. J. Emery and S. A. Kivelson, *J. Low Temp. Phys.* **117**, 189 (1999).

18. A. Gupta, R. Lal, A. Sedky, A. V. Narlikar and V. P. S. Awana, *Phys. Rev.* **B61**, 11752 (2000).
19. A. Gupta, A. Sedky and A. V. Narlikar, to be published.
20. Y. X. Jia, J. Z. Liu, A. Matsushita, M. D. Lan, P. Klavins and R. N. Shelton, *Phys. Rev.* **B46**, 11745 (1992).
21. R. J. Cava, B. Batlogg, K. M. Rabe, E. A. Rietman, P. K. Gallagher and L. W. Rupp Jr., *Physica* **C156**, 523 (1988).
22. G. Bottger, I. Magelschots, E. Kaldis, P. Fischer, Ch. Kruger and F. Fauth, *J. Phys. Condens. Matter* **8**, 8896 (1996).
23. J. C. Phillips, *Proc. Natl. Acad. Sci. (USA)* **94**, 12774 (1997).
24. K. Takenaka, K. Mizuhashi, H. Takagi and S. Uchida, *Phys. Rev.* **B50**, 6534 (1994).
25. T. R. Chien, W. R. Datars, J. Z. Liu, M. D. Lan and R. N. Shelton, *Physica* **C221**, 428 (1994).
26. H. A. Blackstead, J. D. Dow, D. B. Chrisey, J. S. Horwitz, M. A. Black, P. J. McGinn, A. E. Klunzinger and D. B. Pulling, *Phys. Rev.* **B54**, 6122 (1996).
27. A. V. Narlikar, A. Gupta, S. B. Samanta, C. Chen, Y. Hu, F. Wandre, B. M. Wanklyn and J. W. Hodby, *Phil. Mag.* **B79**, 717 (1999).